

A Methodology for Empirical Analysis of Brain Connectivity through Graph Mining

Jiang Bian*, Josh M. Cisler[†], Mengjun Xie[‡], George Andrew James[†], Remzi Seker[‡], and Clinton D. Kilts[†]

*Department of Biomedical Informatics

[†]Brain Imaging Research Center, Psychiatric Research Institute
University of Arkansas for Medical Sciences, Little Rock, Arkansas 72205

[‡]Department of Computer Science
University of Arkansas at Little Rock, Little Rock, Arkansas 72204

Abstract—Graph theoretical analysis has been applied to both structural and functional brain connectivity networks and has helped researchers conceive the effects of neurological and neuropsychiatric diseases including Alzheimer and Schizophrenia. However, existing graph theoretical approaches to brain connectivity networks simply assume that temporal correlations between brain regions are stable during the entire timeseries under consideration, and only focus on high-level network topological characteristics such as degree distribution. To advance the understanding of brain connectivity networks at a fine granularity, we propose a new method that can help discover connectivity-oriented insights from a time series of brain connectivity networks. In particular, our method is capable of identifying (1) strong correlations, which are represented as frequent edges in brain connectivity networks, for each individual subject, and (2) frequent substructures, which are connected components appearing frequently in brain connectivity networks, for a group of subjects. We apply the method to a data set of 38 subjects that were involved in a study of early life stress on depression development. Our findings have been echoed by the domain experts in terms of their clinical implications.

Index Terms—brain connectivity, computational neuroscience, graph theory, graph mining, frequent itemset mining

I. INTRODUCTION

Graph theoretical analyses of both structural and functional human brain networks have been rapidly applied to the understanding of human brain network organizations [1] [2] [3]. Previous studies have found that both structural and functional brain networks resemble features of complex networks such as small-world topology [4] [5], scale-free degree distribution [6], highly connected hubs with high degree or high centrality [7], and modularity [8] [9]. However, most of the previous studies mainly focus on understanding human brain networks through measuring network characteristics on a small scale. Investigation of the correlation between a subject's brain connectome and her clinical conditions still remains largely untouched.

Network characteristics such as mean clustering coefficient, path length, degree distributions, and robustness have been used to capture the differences between diseased subjects and healthy control subjects in Alzheimer [10] and Schizophrenia [11]. However, to simplify analysis, existing graph theoretical approaches (e.g., [12]) to brain connectivity networks do not take the stability of correlations into consideration, assuming

that the temporal correlations between brain regions are stable across the entire timeseries. Moreover, these approaches are not able to discover fine-grained knowledge that exists at correlation level instead of network level. For example, strong correlations in neural network operations, which are of high interest for neuroscientists, cannot be identified by using existing approaches.

In this paper, we propose a new brain network analysis method that can help discover connectivity-oriented insights from a time series of brain connectivity networks. Our method focuses on identifying strong edges (i.e., correlations) that repeatedly appear in brain networks of a subject over time and frequent substructures that are commonly shared by a group of subjects with the same clinical conditions, aiming to provide a microscopic view of important areas in brain networks. Specifically, we use frequent edgesets mining to find frequent substructures. We apply the method to a real-life data set to study the effects of early life stress (ELS) on depression development. Our initial results have triggered great interests from clinical psychiatrists as they find that the frequent substructures derived from the data set exhibit functional modules of brain networks, shedding light on their understandings of brain networks.

ELS includes a wide range of stressors occurring before sexual maturation such as physical and sexual abuse, neglect, and malnourishment. ELS can have profound long-term effects on the development of the central nervous system and its regulation of basic psychology function. ELS can lead to later cognitive impairment. And, ELS is widely documented to increase risk for depression [13]. The neurobiological consequences of stress exposure also involves dysfunction of neural networks mediating cognitive and affective processes [14]. Stresses during infancy may result in deficits in communication between brain cells, memory loss and impaired cognitive abilities that manifest later in life, such as the development of depression [15]. Both ELS and depression might be conceived as a disorder of connectivity between components of brain networks. Presumably, ELS has a high risk of developing depression in later life, and functional brain connectivity network should show some distinct topological characteristics associated with ELS. However, under certain circumstances, a subject can be resilient to the impact of ELS on depression de-

velopment. Even though, a depression resilient subject's brain connectome might show noticeable feature differences from depressed subjects or healthy subjects. In this work, we tested this hypothesis by constructing and comparing functional brain network topologies among different subject groups derived from resting-state functional MRI (fMRI) timeseries.

The rest of the paper is organized into four sections. In the next section, we discuss the background of the study: a) functional and structural brain connectivity and graph theoretical analysis; b) frequent itemset mining and graph mining. In section III, we present our methods from converting subjects' fMRI images to functional brain connectivity graphs, to mining for common substructures and inducing signature graphs. Results and their clinical implications are discussed in section IV. Finally, we conclude with the importance of developing a such general framework for brain connectivity analysis and its potential impacts in the future.

II. RELATED WORK

A. Brain connectivity and graph theory

There are two types of brain connectivity networks: structural network and functional network [16] [1] [5]. Structural networks represent anatomical and physiological associations among different brain elements. This can be achieved by examining the white matter connections among gray matter regions from diffusion tensor image (DTI) data. Functional connectivity indicates the statistical functional association or dependency among individual neurons or brain regions. Functional brain networks can be obtained through measuring temporal correlations between spatially remote neural events based on functional magnetic resonance imaging (fMRI), electroencephalography (EEG), magnetoencephalography (MEG), or multielectrode array (MEG) data.

In this paper, we focus on functional brain connectivity networks obtained from fMRI data. fMRI has been widely used to detect the changes of regional brain activity through their effects on blood flow and blood oxygen consumptions. As a neuronal activity requires glucose and oxygen from the blood stream, it will result in a noticeable change of the local ratio of oxygenation and generate the markers of blood oxygen level-dependent (BOLD) signals for fMRI. The temporal correlations between defined regions of interest (ROIs) can then be calculated by measuring the linear dependence of the signal strengths between two ROIs. In this study, we use the Pearson product-moment correlation coefficient (PMCC) to measure the strength of connection between two ROIs. Other correlation measurement approaches including lag correlation, mutual information, and peak correlation can also be used to measure the dependency between two variables from time series [17].

Using the matrix of correlation coefficients, an undirected graph $G = (V, E)$ of degree $n = |G|$ (i.e. number of vertices/nodes), can be defined to represent the functional brain connectivity network, where a node/vertex of the graph represents a ROI or a neuron and an edge represents a connection/correlation between two nodes and thus indicates

the functional connectivity. Such an abstraction eases the application of Graph theory in quantitative investigation of the topological organization of brain networks. Recent studies have found that both structural and functional brain connectivity networks exhibit properties similar to other complex networks. For example, the small-world phenomenon (i.e. nodes are locally clustered and large networks can be traversed, on average, in a small number of steps) exists in both human brain networks [18] and social networks [19]. For a brain network, a number of network metrics can be measured to analyze its network properties including 1) node degree, degree distribution and assortativity; 2) clustering coefficient and motifs; 3) path length and efficiency; 4) connection density or cost; 5) hubs centrality and robustness; and 6) modularity. Such analyses not only advance our understanding of human brain organizations, but also promote the study of comparing brain networks between diseased patients and healthy subjects to provide more accurate clinical decision support [10] [11].

B. Frequent itemset mining and graph mining

Mining frequent items to find association rules has been extensively studied since the work by Agrawal *et al.* [20]. Association rules can be used to discover the shopping patterns from massive amounts of sales data, which can then be used as the basis of decision making in various activities such as advertising, product placement, etc. An association rule, such as $\{onion, hamburger, meat\} \rightarrow \{potato, chip\}$ demonstrates the customer buying behavior. Frequent sets of products in sales transaction data describe how often items are purchased together.

Formally, let $I = \{i_1, i_2, \dots, i_m\}$ be a set of items. Let D be a collection of transactions, where each transaction $T = (tid, I_{tid})$ has a transaction id tid and a set of items $I_{tid} \subseteq I$. The *support* of a set (X) in D is the number of transactions that contains item set X . A set X is called *frequent* if its support is no less than a given *minimal support* ($minsup$). The *relative minimal support* r_{minsup} is defined as

$$r_{minsup} = minsup/|D|,$$

indicating the probability of set X occurring in all D . The problem of frequent itemset mining is to find all X in

$$F(D, minsup) = \{X \subseteq I | support(X, D) > minsup\}.$$

To go one step further, we can then look for association rules. An association rule is an implication of $X \rightarrow Y$, where $X \subset I, Y \subset I$, and $X \cap Y = \emptyset$. We say that an association rule $X \rightarrow Y$ has *confidence* c , if $c\%$ of transactions in D that contain X also contain Y . For the purpose of this study, we only mine frequent itemsets.

The search space of frequent itemset mining on a set of unique items I contains exactly $2^{|I|}$ different sets. If I is large enough, it is computationally hard to find the supports of all sets over a database D . Therefore, we often just look for closed itemsets and maximal itemsets. A frequent itemset is called *closed* if no superset has the same support. And a

frequent itemset is called *maximal* if no superset is frequent (i.e., exceeding the minimum support).

In graph theoretical analysis, we are often interested in finding frequent subgraphs. For example, in [21], biologists are interested in identifying functional modules and evolutionarily conserved subnetworks from biological networks. Frequent subgraph mining is similar to frequent itemset mining. Given a graph dataset, $D = \{G_0, G_1, \dots, G_n\}$, $support(g)$ is the number of graphs (in D) in which g is a subgraph. The problem of frequent subgraph mining is to find any subgraph g that has $support(g) \geq minsup$. One of the key differences between frequent subgraph mining and frequent itemset mining is to identify *isomorphism* in graphs. However, in our study, we do not consider isomorphic subgraphs, since each ROI is uniquely labeled.

In recent years, solutions on frequent itemset mining (e.g., apriori [20], eclat [22], and fp-growth [23], etc.) and frequent subgraph mining (e.g., AGM [24], FSG [25], and gSpan [26], etc.) have been well explored.

III. METHODS

A. Subject grouping, fMRI data acquiring and data preprocessing

In total 38 subjects have been scanned, and all the subjects are female. Each individual's ELS and depression were characterized by structured interview for Clinical Disorders (SCID) and Early Trauma Inventory (ETI) with trained clinical staff. In addition, all participants completed the Childhood Trauma Questionnaire (CTQ) and Hamilton Depression Scale (Ham-D) to further characterize their ELS histories and current major depressive disorders (MDD). Current or past diagnoses of MDD were determined based on the SCID; ELS history was determined by the ETI and CTQ. 38 subjects were split into three subject groups: 1) a healthy control group (13 subjects), in which subjects had neither ELS nor observation of depression; 2) a resilient group (9 subjects), in which subjects had ELS but did not develop depression symptoms; and 3) a ELS-depression group (16 subjects), in which subjects had ELS and were diagnosed with depression.

Image acquisition was performed using a 3.0 T Siemens Magnetom Trio modality with a Siemens transmit-receive head coil. Anatomic images were acquired at $1 \times 1 \times 1 \text{ mm}^3$ resolution with an MPRAGE sequence as $176 \times 1 \text{ mm}$ thick slices with the following parameters: $FOV 224 \times 256 \text{ mm}$, $TR 2600 \text{ ms}$, $TE 3.02 \text{ ms}$, $FA 8^\circ$. Functional images were acquired with a z-saga sequence 42 to minimize artifact in the medial prefrontal and orbitofrontal cortex due to sinus cavities. Z-saga images were acquired at $3.4 \times 3.4 \times 4 \text{ mm}^3$ resolution in 20 4 mm thick axial slices with the following parameters: $FOV 220 \times 200 \text{ mm}$, $TR 2020 \text{ ms}$, $TE1/TE2 30/66 \text{ ms}$, $FA 90^\circ$. In each session, 210 planar images depicting BOLD responses were acquired with a 2.02 s TR, total duration 7.2 minutes. During the resting-state scan, participants were instructed to lie passively in the scanner and to refrain from thinking about anything specific.

Images first underwent slice timing and motion correction (i.e., corrected for head movement by realignment and regression), and low frequency Fourier bandpass ($0.009 - 0.08 \text{ Hz}$) filtering, then were spatially smoothed to a 6 mm FWHM Gaussian filter, and finally were normalized to the MNI 452 template brain. White and grey matter voxels were segmented using FSL, and noise from white matter voxels was regressed out of the time courses from gray matter voxels.

Certain neural regions are more important than others for emotion processing and emotion regulation. Many studies in neuroscience field have consistently reported such findings among healthy individuals, individuals exposed to ELS, and individuals with MDD [27] [28] [29]. Therefore, we selected 21 well-studied ROIs (see Table I), which have emotion processing and emotion regulation impacts on both healthy and depressed populations [27] [30] [31] [28], to form an emotion regulation network.

TABLE I
SELECTED ROIS IN THE EMOTION REGULATION NETWORK.

| Region of Interest | Description |
|--------------------|---|
| lHPC | Left hippocampus |
| rHPC | Right hippocampus |
| rAMY | Right amygdala |
| lAMY | left amygdala |
| rDFC | Right dorsal lateral prefrontal cortex |
| lDFC | Left dorsal lateral prefrontal cortex |
| rT | Right thalamus |
| lT | Left thalamus |
| lC | Left caudate |
| rC | Right caudate |
| sACC | Subgenual anterior cingulate cortex |
| rACC | Rostral anterior cingulate cortex |
| dACC | Dorsal anterior cingulate cortex |
| mFC | Medial prefrontal cortex |
| vmFC | Ventral medial prefrontal cortex |
| lvFC | Left ventral lateral prefrontal cortex |
| rvFC | Right ventral lateral prefrontal cortex |
| raI | Right anterior insula |
| laI | Left anterior insula |
| rpI | Right posterior insula |
| lpI | Left posterior insula |

Time courses were first extracted from 6 mm sphere ROIs centered at the coordinates of each node for each individual and then averaged across voxels within an ROI, which results in a 21×210 ($ROI \times TPs$) matrix for each individual. In the matrix, each column is an ROI, each row is a time point (TP), and the value of each cell indicates the activity strength of a specific ROI at a specific time point.

B. Constructing functional brain connectivity graphs

In this study, we use the Pearson product-moment correlation coefficient (PMCC) of the time courses to measure the linear dependency (correlation) between two ROIs. The PMCC is calculated based on two variables' covariance, defined as

$$\rho_{X,Y} = E[(X - E[X])(Y - E[Y])]/\sigma_X\sigma_Y \quad (1)$$

where E stands for the mathematical expectation, and σ_X and σ_Y are the standard deviations of X and Y , respectively. The product of PMCC yields a value between -1 and $+1$

inclusive (i.e., $-1 \leq \rho_{X,Y} \leq +1$). A value of +1 indicates a perfect positive linear correlation between X and Y while -1 indicates a perfect negative linear correlation. By calculating the PMCC for every pair of ROIs based on the extracted brain activity time courses, we generate a correlation matrix (21×21) for the 21 ROIs. The matrix is symmetric and the values in the main diagonal are not interested as those values indicate the correlation of an ROI to itself.

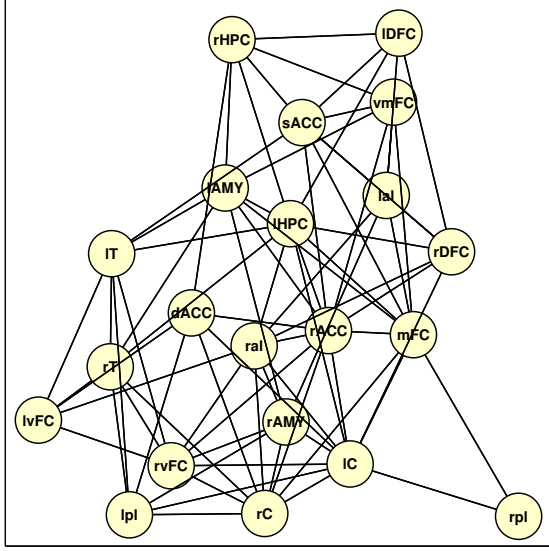


Fig. 1. A sample functional brain connectivity graph that depicts a subject's emotion regulation network.

We can then derive a binary adjacency matrices from the correlation matrices. Two ROIs will be regarded as adjacent to each other and connected via an edge in the connectivity graph, if the two ROIs are highly correlated (either positive or negative). For an adjacency matrix, the value of its entries is either 1 or 0, where 1 indicates the existence of a connection/edge and 0 indicates nonexistence. Formally,

$$A(i, j) = \begin{cases} 1 & \text{if } |\rho_{i,j}| \geq T \\ 0 & \text{if } |\rho_{i,j}| < T \end{cases}, \quad (2)$$

where $A(i, j)$ stands for the value of entry $[i, j]$ in an adjacency matrix, $\rho_{i,j}$ is the correlation value in the corresponding correlation matrix, and T is the given threshold. From an adjacency matrix we can easily construct an undirected graph of brain connectivity network. Each node/vertex in the graph represents an ROI and two ROIs are directly connected if their entry value is 1 in the matrix.

The decision of the value of T is based on the density of a graph. The graph density is defined as the number of edges divided by the total number of possible edges. For an undirected graph $G = (V, E)$ of degree $n = |G|$,

$$density = \frac{|E(G)|}{n(n-1)/2}. \quad (3)$$

Aligned with previous research [11], the graph *density* is set in the range $[0.37, 0.50]$. A graph tends to be fragmented if *density* is smaller than 0.37, and it may not represent a biological system if *density* is larger than 0.50. Clearly, a lower T incurs more correlations and thus more edges, resulting a higher *density* of the graph.

Figure 1 shows an example brain connectivity graph using the selected 21 ROIs with *density* = 0.37.

C. Mining for strong-edges graphs

Visualizing brain networks through functional brain connectivity graphs is very helpful for neuroscientists to understand and analyze the effects of diseases [10] [11]. However, there are two limitations in the existing approaches. First, generated connectivity graphs usually are very complex, full of connections and hard to make comparisons for either between-group subjects or in-group subjects (e.g., see Figure 2). Second, a correlation is decided over the entire timeseries, which assumes that temporal relations between brain regions are quite stable over time. However, it is likely that the assumption is not true [32].

To help better understand functional brain networks, we propose a method that can generate strong-edges graphs from basic functional brain connectivity graphs. The method considers the frequency with which connections between brain regions occur over time and regards the connections that occur frequently as "strong" and important to the function of the overall network. By considering only strong connections, the method can effectively prune the network and reveal patterns of communication across distributed brain regions that define a functional neural network.

We define the strength of an edge (i.e., a correlation between two ROIs), denoted by $S_{e_{i,j}}$ ($1 \leq i \leq |ROI|$, $1 \leq j \leq |ROI|$, and $i \neq j$), as the frequency of its appearance across all the brain connectivity graphs generated from the scan and use it to derive strong edges. The scan on each individual took 7.2 minutes and has 210 time points (TP). We divide the 210 TPs into 41 groups, where each group contains ten TPs. For data smoothing purpose, two consecutive groups have five TPs in common. That is,

$$\begin{aligned} TPG_1 &= [TP_1, TP_2, \dots, TP_{10}], \\ TPG_2 &= [TP_6, TP_7, \dots, TP_{15}], \\ &\dots \\ TPG_{41} &= [TP_{201}, TP_{202}, \dots, TP_{210}]. \end{aligned}$$

In general,

$$TPG_m = [TP_{(m-1) \times step + 1}, \dots, TP_{(m-1) \times step + n}], \quad (4)$$

where TPG_m is the m -th group, TP_i is the i -th TP, and $|TPG|$ is total number of groups. Apparently, $|TPG| = \lfloor (|TP| - n) / step \rfloor + 1$. In this study, we set $step = 5$ and $n = 10$.

We create a correlation matrix and its connectivity graph from each group TPG_m . The strength of an edge $e_{i,j}$ for one

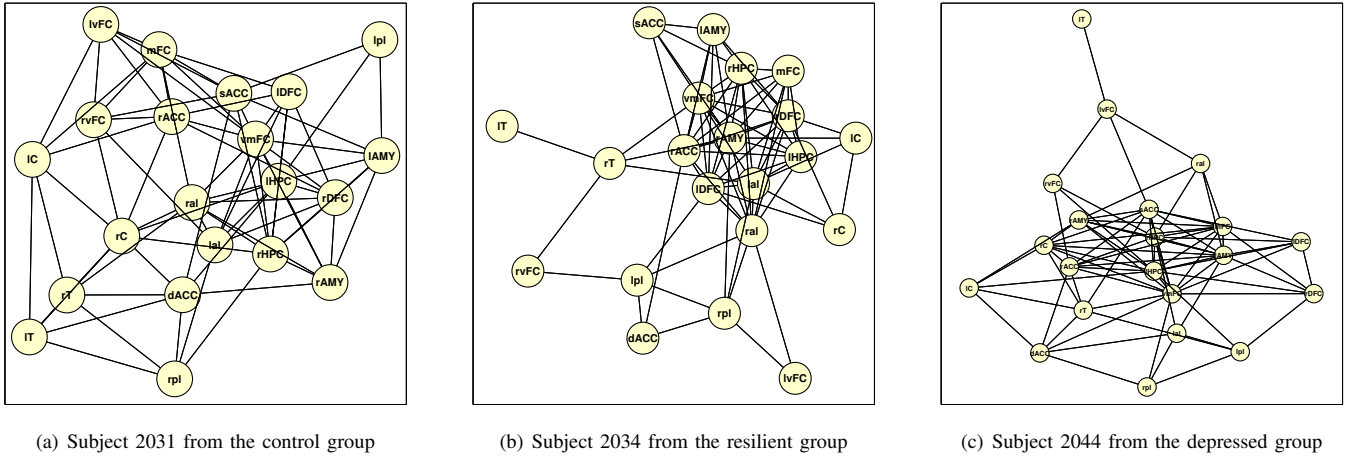


Fig. 2. Functional brain connectivity graphs of three subjects, randomly picked from each clinical group.

subject is defined as

$$S_{e_{i,j}} = |e_{i,j}|/|TPG|, \quad (5)$$

where $|e_{i,j}|$ is the number of graphs that contain edge $e_{i,j}$ and $|TPG|$ is the total number of graphs (i.e., 41 in our study).

Strong edges are those edges whose strengths are no smaller than the predefined minimal support S_{minsup} ($S_{minsup} \in [0, 1]$). Figure 3 shows a strong-edge graph for subject 2031, where $density = 0.42$ and $S_{minsup} = 52\%$. Compared to the original connectivity graph of the same subject in Figure 2(a), the strong-edges graph focuses on edges more frequently observed within operation of the network and therefore increases interpretability by decreasing the total number of edges considered. For example, we can immediately see a clustering effect in Figure 3. Nodes IT, rT, vmFC, mFC, and ral form one cluster, and nodes laI, dACC, rC, IHPC, rHPC, rpl, and rDFC form the other cluster. The two clusters are connected through ral and laI.

D. Frequent edgeset mining and mining for common substructures

We use frequent itemset mining technique to extract a set of key substructures from the individuals' brain connectivity graphs of a subject group. In the context of frequent edgeset mining, given a graph $G = (V, E)$ of degree n , let D be a collection of transactions, where each transaction $T = (tid, E_{tid})$ has a transaction id tid and a set of edges $E_{tid} \subseteq E$. The *support* of a set $X \subseteq D$, denoted by $support(X, D)$, is the number of the transactions that contain edgeset X . A set X is called *frequent* if its support is no less than a given *minimal support* ($minsup$). We define the *relative minimal support* (r_{minsup}) as $r_{minsup} = minsup/|D|$ and use it to indicate the frequency of set X occurred in all transactions. We also restrict the size of X to be larger than $minsize$. The problem of frequent edgeset mining is to find all the subsets X with large enough support and size, that is, to compute the set $\{X \subseteq D | support(X, D) \geq minsup, |X| > minsize\}$.

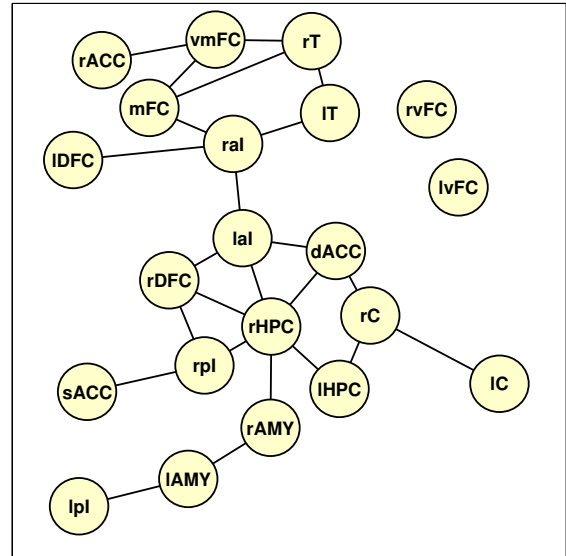


Fig. 3. A sample of a graph that contains only strong edges for subject 2031.

In our study, we define a transaction T as a set of unique edges from each time point group graph of a subject. Aligned with our previous settings (i.e. $step = 5$ and $n = 10$), 210 time points are split into 41 groups. For each group, we can generate a connectivity graph; and we consider each graph of the time point group as a transaction. Using frequent edgeset mining, we can extract frequent substructures (edgesets) of a subject group. Figure 4 shows four different substructures extracted from the healthy control group (i.e. 13 subjects, and $13 \times 41 = 533$ transactions) with the following setting $density = 0.50$, $r_{minsup} = 15\%$, and $minsize = 5$.

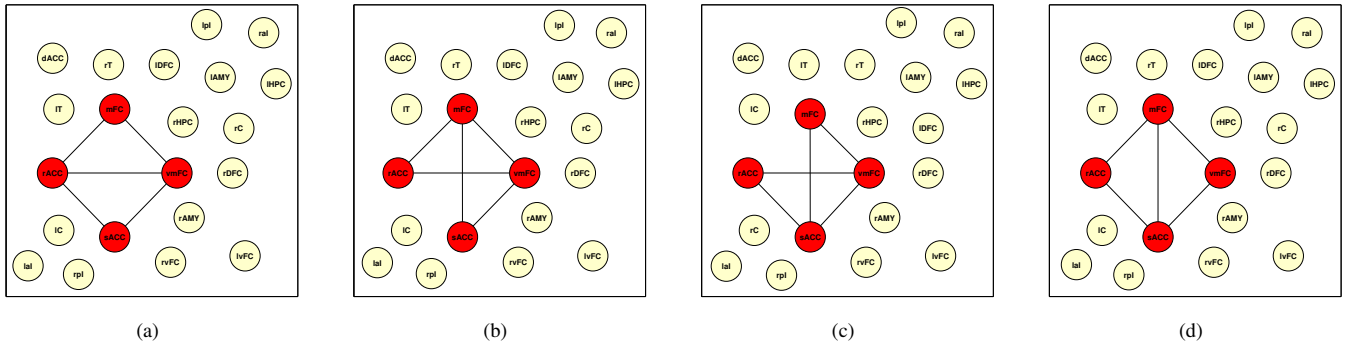


Fig. 4. Samples of frequent substructures extracted from the healthy control group.

IV. RESULTS AND DISCUSSION

The purpose of this study is to explore new approaches to enriching the understanding of human brain networks and discovering insights from them. Traditional graph theoretical approaches (e.g., [12]) to analyzing fMRI data suffer from a) assuming temporal stability across the entire timeseries and b) neglecting to differentiate between commonly used edges and infrequently used ones in neural network operation. In contrast, our approaches focus on strong connections between well-defined ROIs. The immediate result is that we are able to generate strong-edges graphs for each subject and make connectivity graphs much more straightforward, so that key characteristics of a network can be easily observed. As shown in Figure 3, it is clear that two clusters are formed, and connected through nodes *ral* and *lal*. Regions within the *ral* cluster are predominantly involved in executive function (*mFC*, *vmFC*), attention (*rACC*) and integrating multimodal stimuli (*rT*, *IT*). Conversely, regions in the *lal* cluster are commonly associated with affect (*IAMY*, *rAMY*, *sACC*), memory (*IHPC*, *rHPC*), interoceptive sensation (*lpl*, *rpl*), sensory and motor gating (*IC*, *rC*) and error processing (*dACC*). Figure 3 thus depicts a rough division of higher-order cognition from sensory and internal monitoring processes, an interpretation aided by the increased modularity of Figure 3 and not readily evident in the network depicted in Figure 2(a). However, this observation is difficult to draw from the original brain connectivity graph for the same subject in Figure 2(a). Moreover, the strong-edges graphs help infer the stability information of a subject's functional brain networks over time. In this study, 210 time points are grouped into 41 groups and a connectivity graph is generated for each group, which is equivalent to taking a snapshot of the functional brain network of a subject at a given frequency along the time course. The frequency with which an edge appears across the snapshots implies the importance (i.e., strength) of the edge for the overall operation of the network.

We use the frequent edgeset mining techniques to discover common patterns/substructures from brain connectivity graphs of all the subjects within the same clinical group. As shown in Figure 4, frequent substructures are extracted from the healthy control group, with $density = 0.50$, $r_{minsup} = 15\%$, and

$minsize = 5$. Successful emotion regulation is a multidimensional and temporally unfolding process. Neurally, emotion regulation has been found to recruit a diverse array of neural regions that mediate cognitive control, conflict monitoring, memory, emotion and saliency processing, and interoceptive awareness and integration. It is interesting to note that when mining frequent substructures, the control group demonstrated a common substructure consisting of the rostral ACC, subgenual ACC, ventral medial PFC, and medial PFC, as these regions have known direct anatomical pathways connecting them to emotion generation regions (e.g., amygdala and hippocampus). The finding that these regions form a common substructure among healthy individuals suggests that these tightly linked nodes act in concert to bias information processing in emotion generation regions.

Moreover, some literatures suggested that the densities of the brain connectivity networks varied among subjects, therefore, the brain network metrics should consider all reasonable densities, from 0.37 to 0.50 (i.e. for example, take the mean of network metrics produced at a range of densities from 0.37 to 0.50 in 0.01 increments) [11]. In our study, we choose to use a higher density value (i.e. 0.50 at most). As mentioned in Section III-B, the threshold T is determined by the target density, a higher density value results in a lower T , and consequently creates more edges in the graph. Also, we can make the conclusion that if an edge exists in a graph generated using a higher T value, the edge should still exist, if we chose a lower T value (i.e. higher density) and use the same correlation coefficient matrix. In summary, for the purpose of mining for frequent edgesets, a high density value preserves all the necessary edges, and prevents information loss.

Although the methods investigated were only tested on functional brain connectivity networks, they should be also applicable on structural networks, because of their similarities in terms of network characteristics.

V. CONCLUSION

In this paper, we have proposed a new methodology in graph theoretical analyses of brain connectivity networks. Different from traditional approaches, our method does not assume

temporal stability of the brain activities over the entire time-series. To help deepen the understanding of brain connectivity networks, our method focuses on identifying strong edges and discovering common subgraph patterns that exist in subjects of the same clinical conditions. By not assuming static functional connectivity, our method allows improved identification of brain states that differentiate clinical populations.

Following current study, we plan to develop a classification system that can accurately identify potential diseased subjects or neurological flaws on a subject. One possible direction is to rank frequent substructures according to their neurological effects on brain networks, and discard low-ranking patterns as outliers.

REFERENCES

- [1] E. Bullmore and O. Sporns, "Complex brain networks: graph theoretical analysis of structural and functional systems," *Nat. Rev. Neurosci.*, vol. 10, pp. 186–198, Mar 2009.
- [2] J. C. Reijneveld, S. C. Ponten, H. W. Berendse, and C. J. Stam, "The application of graph theoretical analysis to complex networks in the brain," *Clin Neurophysiol*, vol. 118, pp. 2317–2331, Nov 2007.
- [3] C. J. Stam and J. C. Reijneveld, "Graph theoretical analysis of complex networks in the brain," *Nonlinear Biomed Phys*, vol. 1, p. 3, 2007.
- [4] D. S. Bassett and E. Bullmore, "Small-world brain networks," *Neuroscientist*, vol. 12, pp. 512–523, Dec 2006.
- [5] O. Sporns, D. R. Chialvo, M. Kaiser, and C. C. Hilgetag, "Organization, development and function of complex brain networks," *Trends Cogn. Sci. (Regul. Ed.)*, vol. 8, pp. 418–425, Sep 2004.
- [6] V. M. Eguiluz, D. R. Chialvo, G. A. Cecchi, M. Baliki, and A. V. Apkarian, "Scale-free brain functional networks," *Phys. Rev. Lett.*, vol. 94, p. 018102, Jan 2005.
- [7] G. Gong, Y. He, L. Concha, C. Lebel, D. W. Gross, A. C. Evans, and C. Beaulieu, "Mapping anatomical connectivity patterns of human cerebral cortex using in vivo diffusion tensor imaging tractography," *Cereb. Cortex*, vol. 19, pp. 524–536, Mar 2009.
- [8] Z. J. Chen, Y. He, P. Rosa-Neto, J. Germann, and A. C. Evans, "Revealing modular architecture of human brain structural networks by using cortical thickness from MRI," *Cereb. Cortex*, vol. 18, pp. 2374–2381, Oct 2008.
- [9] L. Ferrarini, I. M. Veer, E. Baerends, M. J. van Tol, R. J. Renken, N. J. van der Wee, D. J. Veltman, A. Aleman, F. G. Zitman, B. W. Penninx, M. A. van Buchem, J. H. Reiber, S. A. Rombouts, and J. Milles, "Hierarchical functional modularity in the resting-state human brain," *Hum Brain Mapp*, vol. 30, pp. 2220–2231, Jul 2009.
- [10] Y. He, Z. Chen, and A. Evans, "Structural insights into aberrant topological patterns of large-scale cortical networks in Alzheimer's disease," *J. Neurosci.*, vol. 28, pp. 4756–4766, Apr 2008.
- [11] M. E. Lynall, D. S. Bassett, R. Kerwin, P. J. McKenna, M. Kitzbichler, U. Muller, and E. Bullmore, "Functional connectivity and brain networks in schizophrenia," *J. Neurosci.*, vol. 30, pp. 9477–9487, Jul 2010.
- [12] M. P. van den Heuvel, C. J. Stam, M. Boersma, and H. E. Hulshoff Pol, "Small-world and scale-free organization of voxel-based resting-state functional connectivity in the human brain," *Neuroimage*, vol. 43, pp. 528–539, Nov 2008.
- [13] C. Heim, P. M. Plotsky, and C. B. Nemeroff, "Importance of studying the contributions of early adverse experience to neurobiological findings in depression," *Neuropsychopharmacology*, vol. 29, pp. 641–648, Apr 2004.
- [14] A. F. Arnsten, "Stress signalling pathways that impair prefrontal cortex structure and function," *Nat. Rev. Neurosci.*, vol. 10, pp. 410–422, Jun 2009.
- [15] T. W. Pace, T. C. Mletzko, O. Alagbe, D. L. Musselman, C. B. Nemeroff, A. H. Miller, and C. M. Heim, "Increased stress-induced inflammatory responses in male patients with major depression and increased early life stress," *Am J Psychiatry*, vol. 163, pp. 1630–1633, Sep 2006.
- [16] D. S. Bassett and E. T. Bullmore, "Human brain networks in health and disease," *Curr. Opin. Neurol.*, vol. 22, pp. 340–347, Aug 2009.
- [17] D. Zhou, W. K. Thompson, and G. Siegle, "MATLAB toolbox for functional connectivity," *Neuroimage*, vol. 47, pp. 1590–1607, Oct 2009.
- [18] R. Salvador, J. Suckling, M. R. Coleman, J. D. Pickard, D. Menon, and E. Bullmore, "Neurophysiological architecture of functional magnetic resonance images of human brain," *Cereb. Cortex*, vol. 15, pp. 1332–1342, Sep 2005.
- [19] S. Wasserman and K. Faust, *Social network analysis : methods and applications*, 1st ed., ser. Structural analysis in the social sciences, 8. Cambridge University Press, Nov. 1994. [Online]. Available: <http://www.worldcat.org/isbn/0521387078>
- [20] R. Agrawal and R. Srikant, "Fast algorithms for mining association rules in large databases," in *VLDB'94, Proceedings of 20th International Conference on Very Large Data Bases, September 12-15, 1994, Santiago de Chile, Chile*, J. B. Bocca, M. Jarke, and C. Zaniolo, Eds. Morgan Kaufmann, 1994, pp. 487–499.
- [21] P. Jia-yang, Y. Lu-ming, W. Jian-xin, L. Zheng, and L. Ming, "An efficient algorithm for detecting closed frequent subgraphs in biological networks," in *BioMedical Engineering and Informatics, 2008. BMEI 2008. International Conference on*, vol. 1, May 2008, pp. 677–681.
- [22] M. Zaki, "Scalable algorithms for association mining," *Knowledge and Data Engineering, IEEE Transactions on*, vol. 12, no. 3, pp. 372–390, 2000.
- [23] J. Han, J. Pei, and Y. Yin, "Mining frequent patterns without candidate generation," in *Proceedings of the 2000 ACM SIGMOD international conference on Management of data*, ser. SIGMOD '00. New York, NY, USA: ACM, 2000, pp. 1–12. [Online]. Available: <http://doi.acm.org/10.1145/342009.335372>
- [24] A. Inokuchi, T. Washio, and H. Motoda, "An apriori-based algorithm for mining frequent substructures from graph data," in *Proceedings of the 4th European Conference on Principles of Data Mining and Knowledge Discovery*, ser. PKDD '00. London, UK: Springer-Verlag, 2000, pp. 13–23. [Online]. Available: <http://portal.acm.org/citation.cfm?id=645804.669817>
- [25] M. Kuramochi and G. Karypis, "Frequent subgraph discovery," in *Proceedings of the 2001 IEEE International Conference on Data Mining*, ser. ICDM '01. Washington, DC, USA: IEEE Computer Society, 2001, pp. 313–320. [Online]. Available: <http://portal.acm.org/citation.cfm?id=645496.658027>
- [26] X. Yan and J. Han, "gspan: Graph-based substructure pattern mining," in *Proceedings of the 2002 IEEE International Conference on Data Mining*, ser. ICDM '02. Washington, DC, USA: IEEE Computer Society, 2002, pp. 721–. [Online]. Available: <http://portal.acm.org/citation.cfm?id=844380.844811>
- [27] R. Elliott, R. Zahn, J. F. Deakin, and I. M. Anderson, "Affective cognition and its disruption in mood disorders," *Neuropsychopharmacology*, vol. 36, pp. 153–182, Jan 2011.
- [28] D. A. Seminowicz, H. S. Mayberg, A. R. McIntosh, K. Goldapple, S. Kennedy, Z. Segal, and S. Rafi-Tari, "Limbic-frontal circuitry in major depression: a path modeling metanalysis," *Neuroimage*, vol. 22, pp. 409–418, May 2004.
- [29] G. A. James, M. E. Kelley, R. C. Craddock, P. E. Holtzheimer, B. W. Dunlop, C. B. Nemeroff, H. S. Mayberg, and X. P. Hu, "Exploratory structural equation modeling of resting-state fMRI: applicability of group models to individual subjects," *Neuroimage*, vol. 45, pp. 778–787, Apr 2009.
- [30] T. Johnstone, C. M. van Reekum, H. L. Urry, N. H. Kalin, and R. J. Davidson, "Failure to regulate: counterproductive recruitment of top-down prefrontal-subcortical circuitry in major depression," *J. Neurosci.*, vol. 27, pp. 8877–8884, Aug 2007.
- [31] S. C. Matthews, I. A. Strigo, A. N. Simmons, T. T. Yang, and M. P. Paulus, "Decreased functional coupling of the amygdala and supragenual cingulate is related to increased depression in unmedicated individuals with current major depressive disorder," *J Affect Disord*, vol. 111, pp. 13–20, Nov 2008.
- [32] C. T. Whitlow, R. Casanova, and J. A. Maldjian, "Effect of Resting-State Functional MR Imaging Duration on Stability of Graph Theory Metrics of Brain Network Connectivity," *Radiology*, Mar 2011.